

**LEAR
CRYSTAL BARREL EXPERIMENT
PS 197**

**SMART
-
SPLIT-OFF RECOGNITION
IN
PURE NEUTRAL EVENTS**

b y

Jürgen E. Salk

**Ruhr-Universität
Bochum**

20.Oct.1991

1. Introduction

One of the most troublesome problems in processing the barrel calorimeter raw data is the occurrence of low energy PEDs which are not due to real particle energy deposits but to spatial fluctuations of the electromagnetic showers produced by an incoming photon. These so-called split-offs are hard to distinguish from low energy photons, so people dealing with calorimeter data are forced to require some severe conditions on their data to accept suitable events for the desired decay-channel.

Two typical procedures are in common:

1. Processing BC-Data with $E_{CLUBC} = E_{PEDBC} = 10$ MeV and requirement of exactly n PEDs ($n = 1,2,3,\dots$) with $E_{PED} > 20$ MeV and no PEDs with $E_{PED} < 20$ MeV.¹
2. Processing BC-Data with $E_{CLUBC} = E_{PEDBC} = 20$ MeV and requirement of exactly n PEDs (standard method).²

E_{CLUBC} is the minimum energy of one cluster. E_{PEDBC} is the minimum energy of the central crystal of one PED (but not for the first PED in a cluster).

I will now summarize the main deficiencies of both methods:

Method 1:

- Voluntary renunciation of events with low energy photons although those events are actually available on DST.
- Insufficient split-off suppression as can be easily seen by the enhancement in the low energy region of the gamma energy spectrum.

Method 2:

- Software-caused nonsensitivity for low energies (No PEDs < 20 MeV are an DST.)
- Neglecting low energy photons lead to a bad pollution of the data by events of higher gamma multiplicities.

¹This method is obsolete.

²This method was already used by K. Peters in his $3\pi^0$ - analysis /1/ and is also used in other analysis works.

In this CB-Note, I want to introduce a method to distinguish split-off PEDs from ordinary PEDs in order to get a better purity of the data sample down to energies of 10 MeV.

The aim of this study is to realize whether the invariant showermass of a cluster shows distinctive properties, which enable the user to recognize split-offs efficiently.

The invariant showermass of a cluster is calculated via

$$R_{\text{mass}} = \sqrt{\left(\sum_{\text{Xtals}} E_i \right)^2 - \left(\sum_{\text{Xtals}} \vec{p}_i \right)^2}$$

where the sum extends over all crystals in the cluster /2/.

Note that the invariant showermass is more than just a measure of the spatial distribution of an electromagnetic shower. It gives information about the shape (the topology) of a cluster and can even be used to identify neutral pions.

2. A short look at the experimental data

An inspection of fig.1, where the invariant showermass is plotted versus the energy of the cluster for all neutral events without regard to the gamma multiplicity, shows the following items. (run 2105 was used.)

- The showermass of clusters with only one PED (fig. 1a)) is always as low as expected.³
- The showermass of clusters including two PEDs (fig. 1b)) shows a steeper increase with rising energy, but there seems to be an amount of clusters showing quite similar characteristics as clusters with only one PED. This clusters are mainly split-offs as will be shown below. Note that the enhancement of the showermass in the region of 140 MeV/c^2 is due to merged π^0 's.
- Inspecting clusters including three PEDs (fig. 1c)) one finds a further slighter increase of the showermass. Clearly most of the clusters show the characteristics of clusters with a lower number of PEDs.

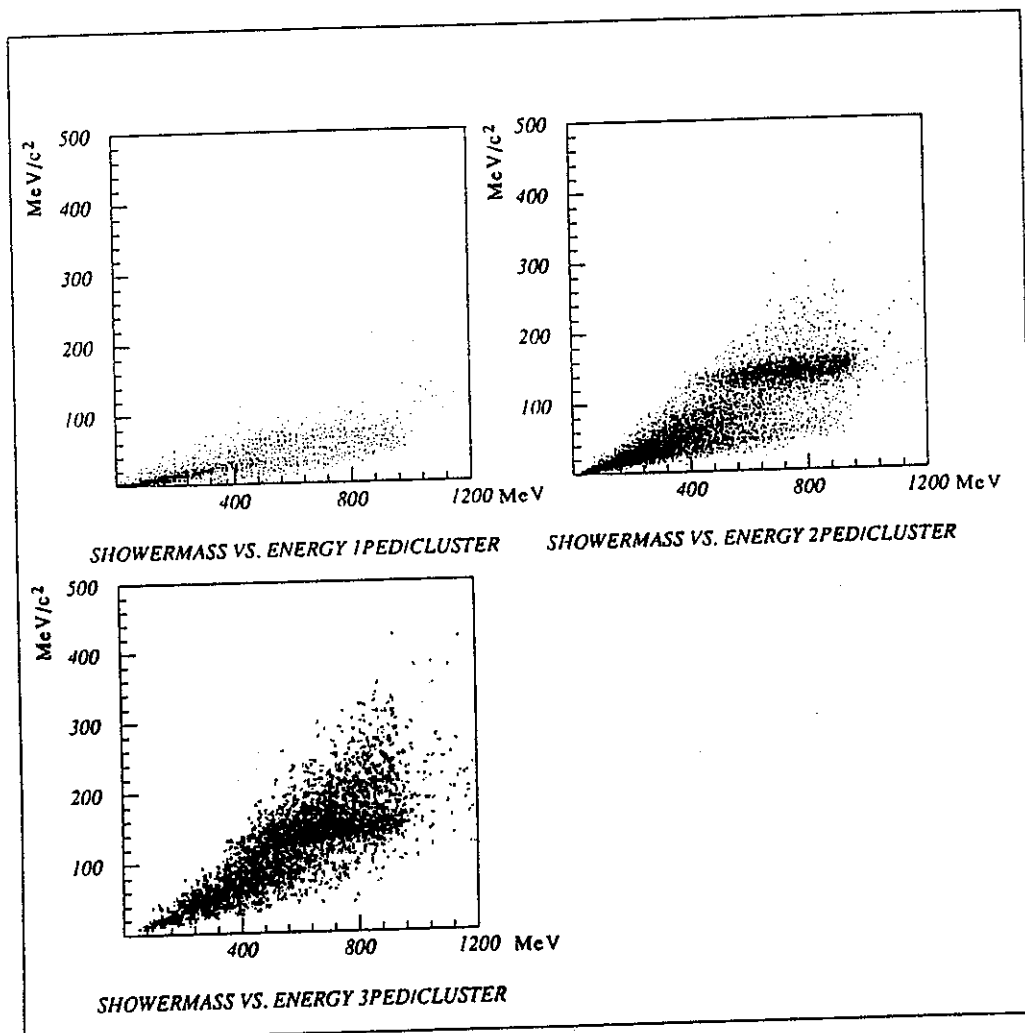


Figure 1 Showermass vs. energy of the clusters

³ Note that the slight increase of the showermass with rising energy is due to a systematical error in the calculation of the showermass [2/].

3. Monte-Carlo-Studies

In order to study the split-off topology Monte-Carlo events of different decay channels were generated (see tab.1).

For the following analysis the data were processed with ECLUBC = EPEDBC = 10 MeV and 20 MeV, respectively.

To make sure that nothing but the behaviour of photons was observed, events with the occurrence of Dalitz decays or with gamma conversion in the PWC, JDC or other passive material were excluded.⁴

The probability for interaction or conversion in passive material was found out to be about 0.06/photon.

Table 1

event type	total number of generated events	events without Dalitz decay	events without conversion in passive material
$\pi^0 \pi^0$	20000	19534	15320
$\pi^0 \eta$	30000	29635	23103
$\pi^0 \omega$	50000	48797	36249
$\eta \omega$	10000	9883	7289
$\pi^0 \pi^0 \pi^0$	10000	9607	6726
$\pi^0 \pi^0 \eta$	10000	9746	6854
$\eta \eta \eta$	10000	10000	6889
$\pi^0 \pi^0 \pi^0 \pi^0$	30000	28511	18198

From the MC generated events, it was possible to tag split-off PEDs in the following way:

An algorithm very similar to the procedure offered in BCMCOR /3/ was used to correlate the generated particles with PEDs found by the offline-analysis software (see appendix I).

The correlation was assumed to be successful if every photon which deposited at least an energy of $1.05 \cdot \text{ECLUBC}$ in the crystals could be correlated with a PED, found by the crystal reconstruction software.

A PED was supposed to be a split-off if it was not correlated with an incoming gamma.

The results are given in tables 2.1 and 2.2. You can compare the different split-off probabilities for ECLUBC = EPEDBC = 10 MeV and 20 MeV, respectively.

⁴ Control plots, where such events were kept looked exactly the same.

See e.g. the two π^0 channel in table 2.1 (ECLUBC = EPEDBC = 10 MeV): 15241 events of the 15320 events without any Dalitz decay or gamma conversion in passive material were found to have full correlation between the incoming generated gammas and the PEDs. 12091 of the events did not show any split-off in the barrel (i.e. every PED was correlated with a gamma). 3150 of the events were found to have one or more split-offs (i.e. remaining PEDs after successful correlation). The split-off probability per photon p was calculated using

$$(1-p)^n = \frac{\# \text{ events without any split-off}}{\# \text{ events with successful correlation}},$$

where n is the gamma multiplicity of the special event type.

event type	successful correlation	events without any split-off	events with split-offs	split-off probability per photon
$\pi^0 \pi^0$	15241	12091	3150	0.057
$\pi^0 \eta$	23012	17744	5268	0.063
$\pi^0 \omega$	35961	27135	8826	0.055
$\eta \omega$	7238	5313	1925	0.060
$\pi^0 \pi^0 \pi^0$	6623	4776	1847	0.053
$\pi^0 \pi^0 \eta$	6743	4775	1968	0.056
$\eta \eta \eta$	6828	4747	2081	0.059
$\pi^0 \pi^0 \pi^0 \pi^0$	17678	11776	5902	0.050

Table 2.1: ECLUBC = EPEDBC = 10 MeV

event type	successful correlation	events without any split-off	events with split-off	split-off probability per photon
$\pi^0 \pi^0$	15320	14731	421	0.010
$\pi^0 \eta$	22979	22210	769	0.008
$\pi^0 \omega$	35668	34159	1509	0.009
$\eta \omega$	7187	6840	347	0.010
$\pi^0 \pi^0 \pi^0$	6514	6064	450	0.011
$\pi^0 \pi^0 \eta$	6664	6140	524	0.014
$\eta \eta \eta$	6823	6155	668	0.017
$\pi^0 \pi^0 \pi^0 \pi^0$	17193	15111	2082	0.016

Table 2.2: ECLUBC = EPEDBC = 20 MeV

An energy cut of 20 MeV (see tab.2.2) on the central crystal of the PEDs seems to be a reasonable cut if one aims only at split-off suppression but we have to take into account that we are no longer able to perceive photons in the energy region between 10 and 20 MeV.

3.1 Analysis of the invariant showermass of the clusters

Have a look at fig.2 where again the showermass is plotted versus the cluster energy. The data was processed with $E_{CLUBC} = E_{PEDBC} = 10$ MeV. On the l.h.s. only clusters were taken, where every PED is correlated with a photon. In the following I will call these clusters 'correct clusters'. On the r.h.s. only clusters containing at least one split-off were taken.

Obviously the energy dependence of the showermass is quite different in the presence of split-offs.

In general, clusters with n PEDs including 1 fake PED turn out to have exactly the same characteristics as correct clusters with $n-1$ PEDs. Note the correspondence between fig.2 d) and 2 a) or between fig.2 f) and 2 c).

Comparing correct clusters and split-off clusters containing the same number of PEDs (compare e.g. fig.2 c) and 2 d)) it seems reasonable to consider an energy dependent cut on the showermass (with respect to the topology of the cluster) to separate clusters with or without split-offs.

Unfortunately, the region where split-offs appear is not completely separated from the region of correct clusters. As a consequence of this overlap (the region between the full and the dotted line in figures 2) it is useful to divide the plane into three parts:

1. Clusters in the region above the full line are assumed to be correct, i.e. no split-offs.
2. Clusters in the region between the lines are ambiguous, i.e. we can not identify them as correct clusters definitely. Events with the occurrence of such dubious clusters should be rejected.
3. Clusters in the region below the dotted line are considered as containing split-offs.

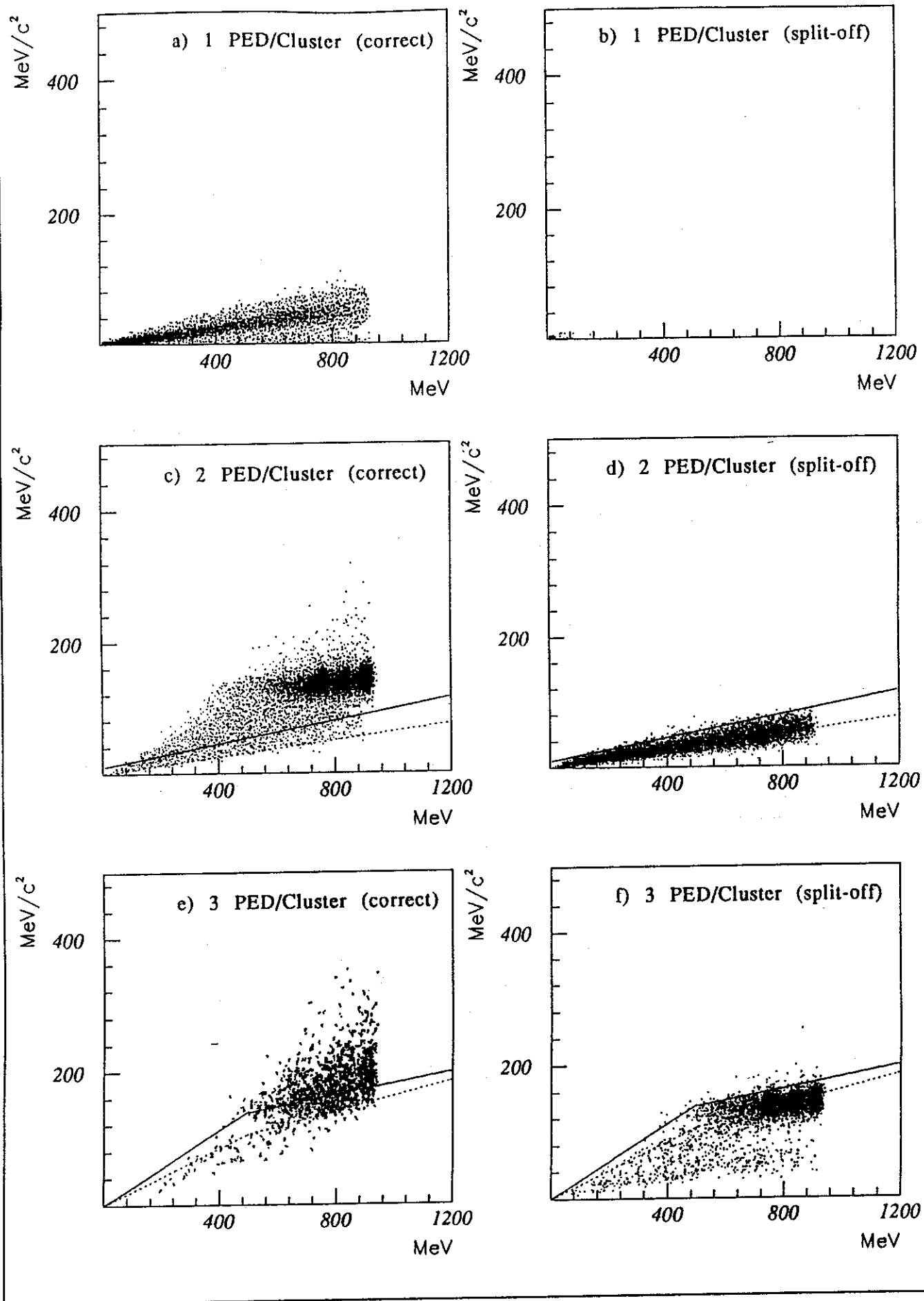


Figure 2 Showermass vs. energy of real clusters

3.2 Analysis of split-off PEDs forming a separated cluster

Monte-Carlo studies showed that about 30 % (!!!) of all split-off PEDs form their own well separated cluster. To reveal such PEDs, every cluster with a single PED (i.e. clusters with only one PED) and a central crystal energy lower than 30 MeV was joined together with the nearest cluster. The resulting 'clusters' are called 'pseudo clusters' to distinguish them from the ordinary real clusters. The invariant showermass of the resulting pseudo clusters was calculated and plotted in the well known fashion in figures 3.

The interpretation of fig.3 a)-f) is quite similar as in the case of real clusters. The characteristics of pseudo clusters is quite similar to the characteristics of real clusters with the same number of PEDs (Compare e.g. fig.3 a) with fig.2 c) or fig.3 b) with fig.2 d).) In fig.3 a) the π^0 signal shows up very clearly again. That is for the case that the gammas of a high energy π^0 did not merge but form two well separated clusters with each of them containing exactly one PED.

Again an energy and topology dependent cut on the showermass of the pseudo clusters provides a chance to separate split-off clusters from correct clusters. Note that this technique enables the user to find out a split-off PED even if it has formed his own well separated cluster.

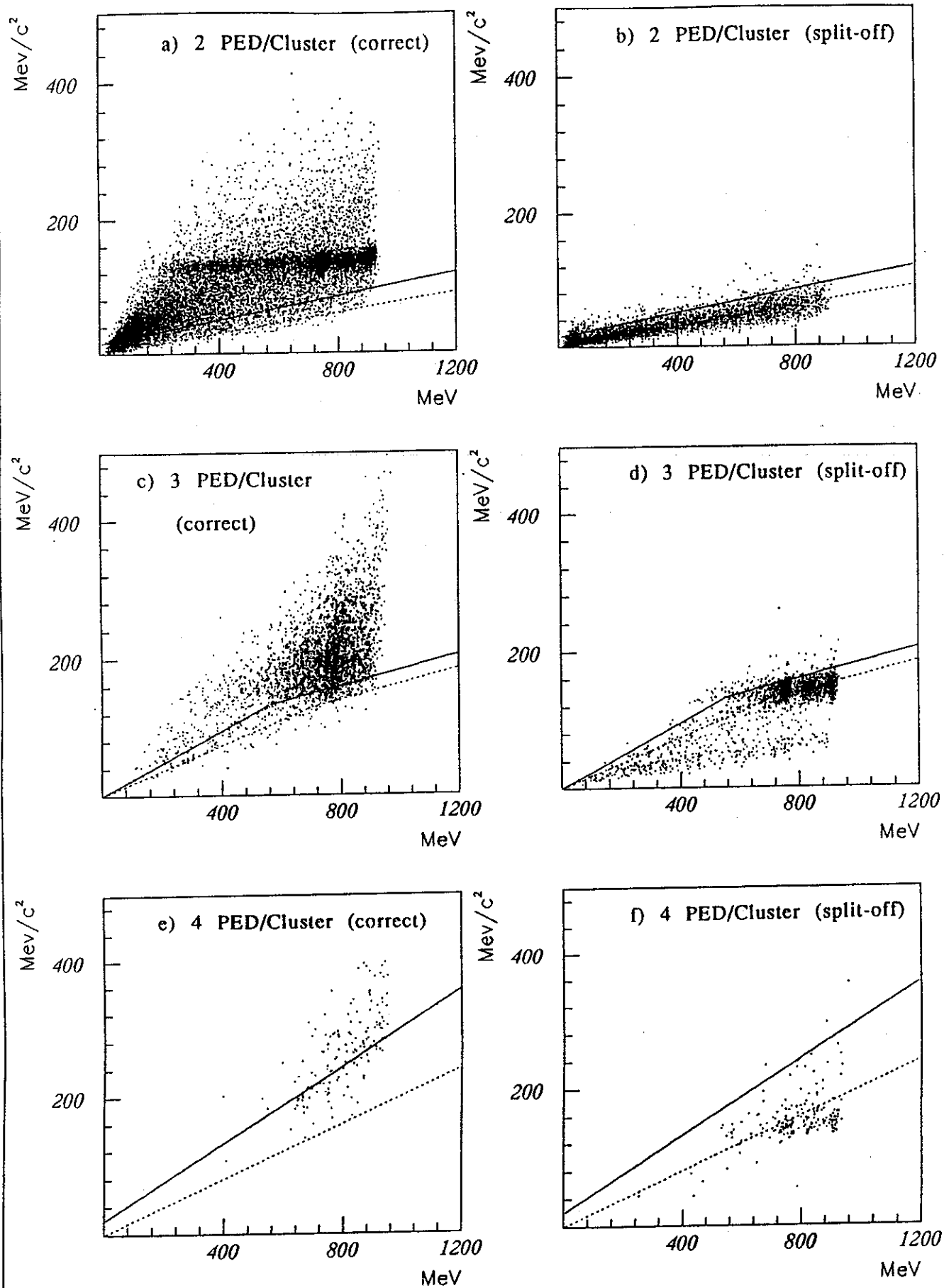


Figure 3 Showermass vs. energy of pseudo clusters

4. Efficiency studies

I will now introduce a method which is called the *SMART* method, because it is based on showermass cuts with respect to the topology of the clusters. The efficiencies obtained by the SMART and our standard method will be compared.

To obtain useful values for the efficiencies the following analysis was done without any restrictions, i.e. events with the occurrence of Dalitz decays or conversion in passive material were no longer excluded.

First I will give a brief description of both methods:

The standard method:

- Processing calorimeter raw data with $ECLUBC = EPEDBC = 20$ MeV
- Reject events with charged tracks in the JDC
- Application of 4C-Fit with a confidence level cut $CUTCL = 0.1$

The SMART method:

- Processing raw data with $ECLUBC = EPEDBC = 10$ MeV
- No charged tracks in JDC
- Application of SMART cuts described below
- Application of 4C-Fit with $CUTCL = 0.1$

Application of SMART cuts means the following way of proceeding:

1. Loop over every cluster containing two or more PEDs:
 - Refuse events with the occurrence of one or more ambiguous clusters (i.e. clusters in the region between the full and the dotted lines in fig.2).
 - Refuse events with the occurrence of clusters containing five or more PEDs.
 - Clusters in the region below the dotted line in fig.2 are assumed to be clusters containing split-offs. In the case of two PEDs per cluster drop the PED with the lowest energy. In the case of three or more PEDs per cluster drop every PED with a central crystal energy lower than 50 MeV (but retain at least one PED).
2. Loop over every cluster containing exactly one PED:
For every PED with a central crystal energy lower than 30 MeV make a pseudo cluster by combining the PED with the nearest cluster. Now repeat the steps described above (replace 'fig.2' by 'fig.3' and '50 MeV' by '30 MeV').

Note that for the case of pseudo clusters a lower energy threshold was used (30 MeV instead of 50 MeV). This is reasonable because Monte-

Carlo studies shows that the central crystal energy is always lower in the case of a well separated split-off PED than in the case that the split-off PED is still joined with its parent cluster. The reason for this is very simple: a well separated split-off PED does not get any energy offset by the spur of its parent cluster.

A detailed list of the two dimensional region cuts used in this analysis and shown in fig.2 and fig.3 is given in appendix II.

The results for the different decay channels are listed in tab.3, where the probability of acceptance is given for the different gamma multiplicities in the hypothesis input. The l.h.s. of the columns show the results for the standard method, the r.h.s show the results obtained by the SMART method.

No.of γ 's	$\pi^0 \pi^0$		$\pi^0 \eta$		$\pi^0 \omega$		$\eta \omega$	
	standard	SMART	standard	SMART	standard	SMART	standard	SMART
1								
2	0.001							
3	0.042	0.022	0.026	0.013	0.001		0.001	
4	0.490	0.472	0.495	0.442	0.047	0.020	0.031	0.015
5	0.026	0.004	0.026	0.004	0.416	0.370	0.425	0.356
6	0.001				0.025	0.005	0.026	0.005
7					0.001			
8								
	$\pi^0 \pi^0 \pi^0$		$\pi^0 \pi^0 \eta$		$\eta \eta \eta$		$4 \pi^0$	
	stand.	SMART	stand.	SMART	stand.	SMART	stand.	SMART
3								
4	0.004	0.001	0.004	0.001				
5	0.071	0.039	0.065	0.035	0.029	0.025		
6	0.349	0.293	0.351	0.291	0.382	0.311	0.012	0.004
7	0.021	0.005	0.022	0.006	0.036	0.006	0.084	0.044
8	0.001		0.002		0.001		0.252	0.180
9							0.023	0.004
10								

Table 3: Probability of acceptance

Imagine you are looking for a five gamma final state, say $\pi^0 \omega$:

The probability for a $\pi^0\omega$ event to be accepted as a five gamma final state turns out to be 41.6 % using the standard method. If one applies the SMART method this probability is 37.0 %.

After such a cursory glance one could draw the conclusion that the standard method yields the better result. But this is an error as can be easily seen by a closer look at the other columns of tab.3 where the potential background channels can be found:

2.6 % of all $2\pi^0$ events occur as a five gamma final state, if one applies the standard method (0.4 % for the SMART method). 7.1 % (!!!) of all $3\pi^0$ events produce background in the five gamma final state (3.9 % for the SMART method). Obviously the background fraction can be drastically reduced by the application of SMART. That's why this method should be preferred to our standard method.

A compressed representation of the efficiencies can be found in fig.4.

The active inefficiency is given in fig.5. The active inefficiency is defined to be the probability for an event to survive a 4C-Fit with an incorrect number of gammas in the hypothesis input. This type of inefficiency is called active because the corresponding events are still taken for the analysis, i.e. the active inefficiency is responsible for the background signal in our data. Note that about 10 percent of all $3\pi^0$ events produce background in other channels (mainly in 5γ final states) if one applies the standard method. This fraction can be reduced by about a factor of 2 if one applies the SMART method.

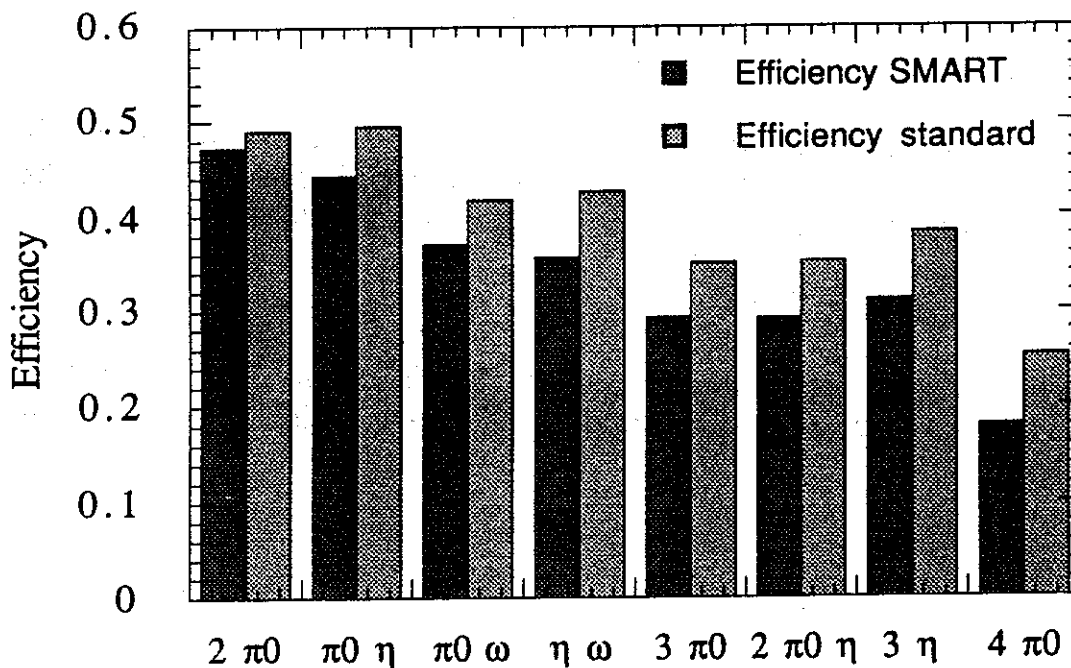


Figure 4

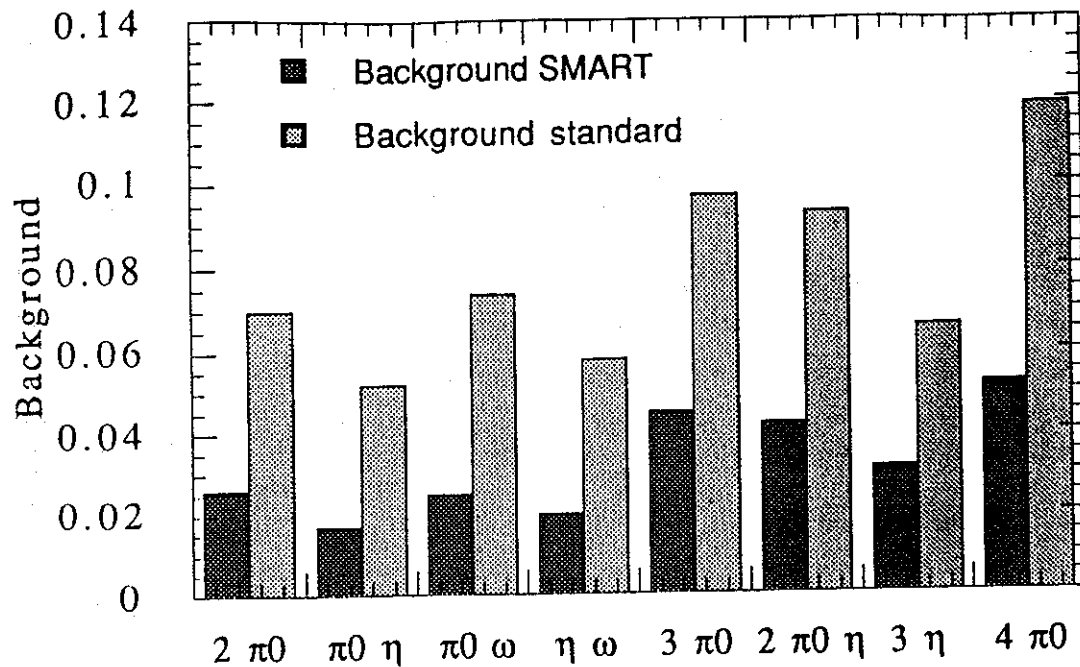


Figure 5

To compare the results of both procedures we define the purity P via

$$P = \frac{N_{\text{Correct}}}{N_{\text{All}}},$$

N_{Correct} = Number of events which survived the 4C-Fit with the correct number of gammas in the hypothesis input

N_{All} = Number of all events which survived the 4C-Fit

The purity for the different event types is given in fig.6. One can easily check, that the SMART method yields an average improvement of the purity by 7.6 percent. This seems not to be an important improvement, but one has to take into account, that gamma energies down to 10 MeV are accessible (possibly 5 MeV).

The background fraction of a special event type is simply $1-P$, plotted in fig.7. It turns out that it is drastically reduced by the application of SMART cuts.

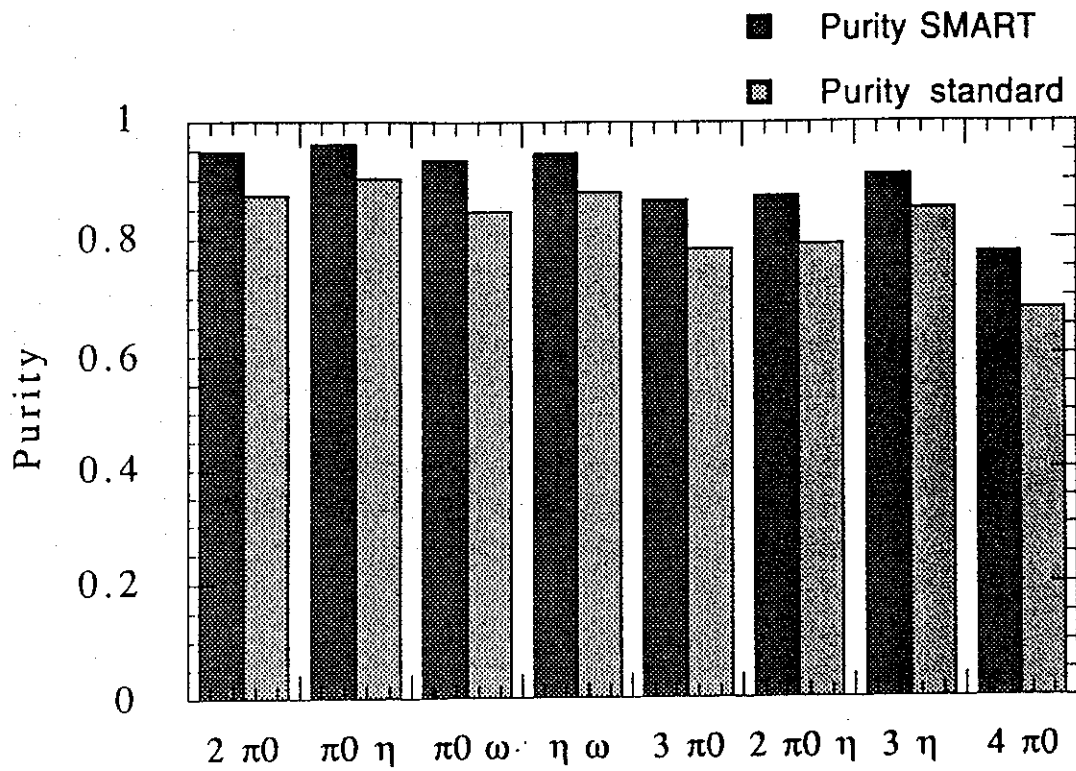


Figure 6

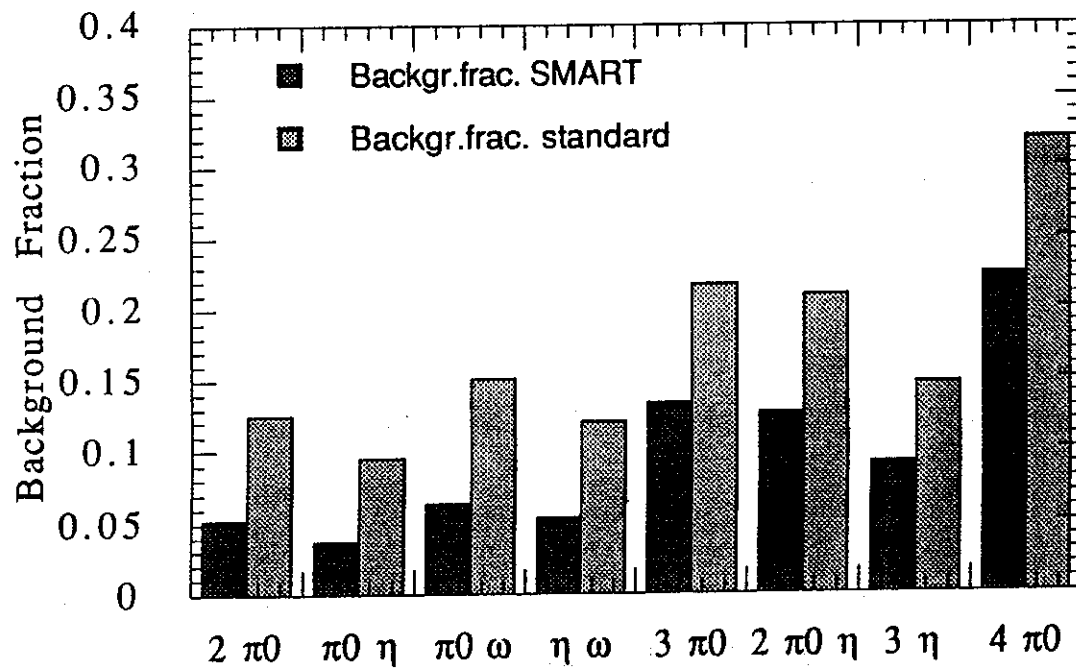


Figure 7

The merits of the methods are again demonstrated in figures 8. Fig.8 a) shows the gamma energy spectrum of all generated decay channels as measured by an ideal gamma-detector, i.e. the original kinematics is taken as generated by GENBOD. In fig.8 b) one can see the results as measured by the Crystal Barrel detector performance using an energy cut of $ECLUBC = EPEDBC = 10$ MeV. The huge peak below 80 MeV is due to split-off PEDs. Fig.8 c) shows the energy spectrum for the same events obtained with an energy cut of $ECLUBC = EPEDBC = 20$ MeV (the standard method). Note that every photon with an energy lower than 20 MeV is lost and you still can not place confidence in the range below 80 MeV. Now have a look at fig.8 d). This is the improved gamma energy spectrum obtained by the SMART method. Compare this with fig.8 a), where the original kinematics is taken. The shape of the spectra are as similar as never obtained by any other procedure (even in the critical range below 80 MeV).

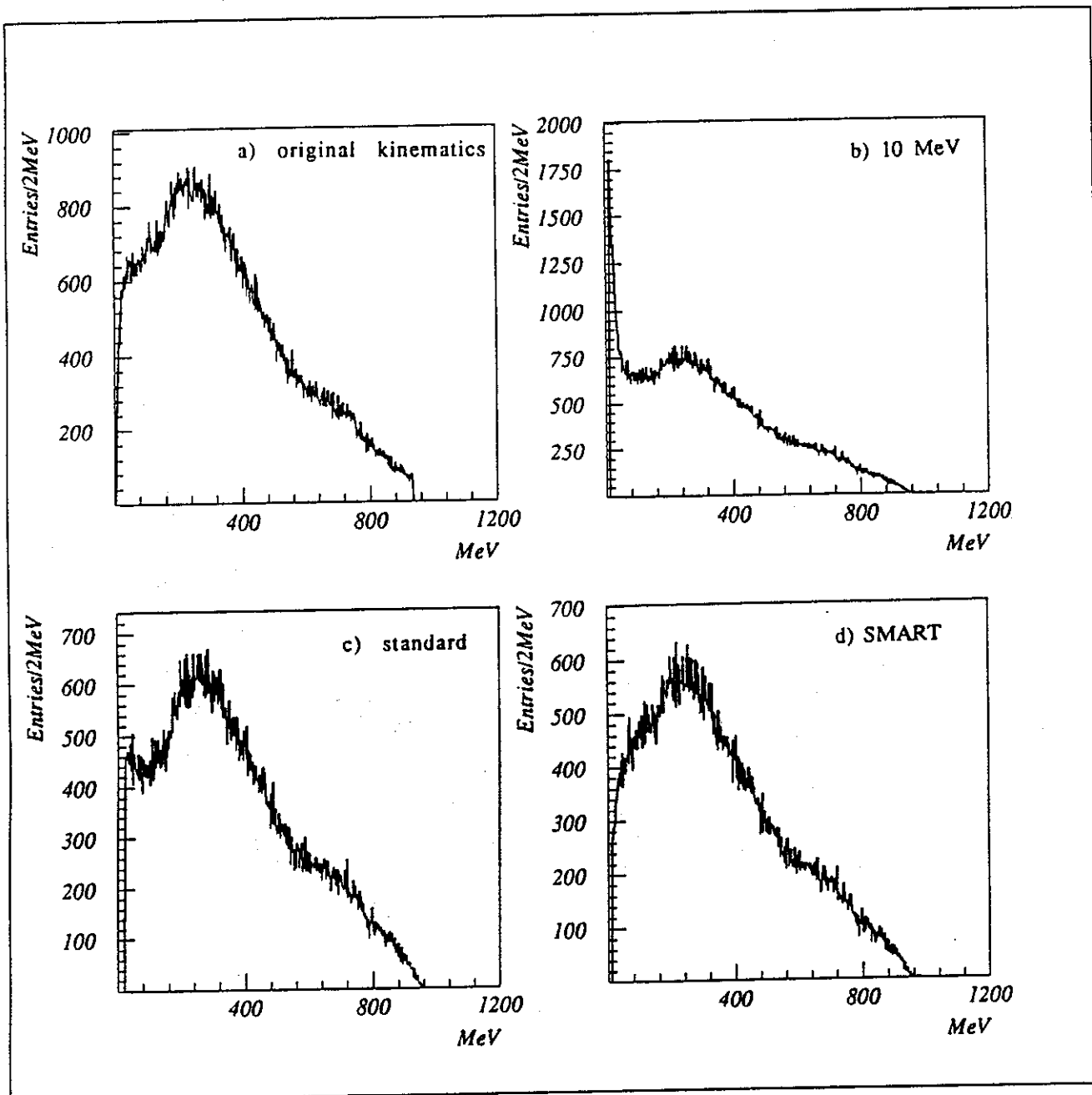


Figure 8

4. Summary

This CB-Note describes an alternative approach to the problem of electromagnetic split-off suppression. A new technique was introduced, which is based on energy dependent cuts on the invariant showermass respecting the topology of the clusters (SMART). Monte-Carlo studies with CBGEANT showed that the SMART method provides an excellent tool for split-off suppression at the Crystal Barrel calorimeter. A comparison between the SMART method and our standard method showed that the SMART method yields much better results in split-off suppression (see tab.3). As the SMART method do not require an increase of ECLUBC and EPEDBC from 10 MeV to 20 MeV, even the background due to lost low energy photons can be drastically reduced by about a factor of 2 (see tab. 3).

The application of the SMART method is vital for special applications, e.g. the research of radiative decays, say $p\bar{p} \rightarrow \gamma X_2(1515)$, where a very strong background due to $p\bar{p} \rightarrow \pi^0 X_2(1515)$ occurs.

One should also consider to use SMART in general applications, because it yields a better purity of our data.

An easy-access version of SMART will be implemented in BCTRAK as soon as possible to make it available for every user.

5. References

- /1/ K. Peters, Beobachtung des $X_2(1515)$ in der Antiproton-Proton-Annihilation in $3\pi^0$, Dissertation, Mainz 1991
- /2/ S. Kelzenberg, Identifizierung von Photonen mit dem Crystal-Barrel-Detektor, Diplomarbeit, Karlsruhe 1990
- /3/ F.-H. Heinsius, T. Kiel, Crystal Data Reconstruction Software, CB-Note Nr.92

Appendix I:

Procedure used to correlate Monte-Carlo particles with PEDs found by the offline analysis software.

```
SUBROUTINE MCCORR (IPA,ITR,EP,NMAX,NCO,NPART,NPEDS)
```

```
Author : F.-H. HEINSIUS 04/10/90
```

```
Modified : Juergen Salk 06/08/91
```

```
SUBROUTINE MCCORR (IPA,ITR,EP,NMAX,NCO,NPART,NPEDS)
```

```
Based on SUBROUTINE BCMCOR.
```

```
Correlation of MC-energy deposition of particles with  
PEDs found after event analysis.
```

```
Based on Algorithm by Reinhard Lekebusch.
```

```
Expected input:
```

```
NMAX = Dimension of IPA,ITR,EP (<= 50)
```

```
Final output:
```

```
IPA(NMAX) = MCtrack#(ped#)
```

```
ITR(NMAX) = ped#(MCtrack#) (0=no corr,-1=no energy,-2 low)
```

```
EP(NMAX) = deposited energy of particle(MCtrack#)
```

```
NCO = Number of correlated peds - particles
```

```
NPART = Number of particles with  $EP * 1.05 > ECLUBC$   
(cluster energy)
```

```
NPEDS = Number of PEDs
```

```
==>Called by : user
```

```
==>Calling : BITOPT
```

```
Correlation of Particles with PEDs
```

```
** COMMONS
```

```
include '/u/juergen/analyse/common.inc'
```

```
** IPHP() = phi of maximum xtal (MCtrack#)
```

```
** ITHP() = theta of maximum xtal (MCtrack#)
```

```
INTEGER NMAX,IPHP(50),ITHP(50),IPA(NMAX),ITR(NMAX)
```

```
INTEGER NCO,NPART,NPEDS,NTRACK,I,LMBEN,IT,IMAX,LM,LMAX,IP
```

```
REAL EP(NMAX),EMAX,EXTL
```

```
*** New event: Clear correlations
```

```
** Number of correlated
```

```
NCO=0
```

```
DO 10 I= 1, MIN(NMAX,50)
```

```
IPHP(I)=0
```

```
ITHP(I)=0
```

```
IPA(I)=0
```

```
ITR(I)=0
```

EP(I)=0
10 CONTINUE

*** direction of particles = direction of maximum xtal

LMBEN = LQ(LRMCB-4)
NTRACK=IQ(LMBEN+1)
NPART=NTRACK

** Loop over all particles (deposited energy in MBEN)
DO 100 IT = 1, IQ(LMBEN+1)

EMAX=0.
IMAX=0

* loop over xtals of particle IT, search maximum xtal

LM=LQ(LMBEN-IT)
EP(IT)=Q(LM+1)
DO 50 I=1, IQ(LM)
EXTL=Q(LM+2*I+1)
IF (EXTL.GT.EMAX) THEN
EMAX=EXTL
IMAX=IQ(LM+2*I)

END IF

50 CONTINUE

* save direction of particle in IPHP, ITHP

IF (IQ(LM).EQ.0) THEN

* this particle deposited no energy

NPART=NPART-1
IPHP(IT)=0
ITHP(IT)=0
ITR(IT)=-1

ELSE

CALL BITOPT(IMAX, IPHP(IT), ITHP(IT))

* CALIBRATION

EP(IT)=EP(IT)
IF (EP(IT)*1.05 .LT. ECLUBC) THEN

* not enough energy for a cluster

NPART=NPART-1
ITR(IT)=-2

END IF

END IF

100 CONTINUE

*** Correlation, if max xtal particle = max xtal PED

NPEDS=IQ(LTBTK+1)

** loop over all particles

DO 210 IT = 1, IQ(LMBEN+1)

** loop over all PEDs

LMAX=LTBTK
IF (LMAX.NE.0) LMAX=LQ(LMAX-1)

200 IF (LMAX .NE. 0) THEN

* max xtal particle = max xtal ped ?

IF ((IPHP(IT).EQ.IQ(LMAX+1)) .AND.
& (ITHP(IT).EQ.IQ(LMAX+2))) THEN

* PED#

IP = IQ(LMAX-5)

* ipa(ip) .ne. 0 : Another particle correlates with ped IP

* itr(it) .ne. 0 : Particle IT deposits not enough energy for ped IP

```

IF ((IPA(IP).EQ.0).AND.(ITR(IT).EQ.0)) THEN
  IPA(IP)=IT
  ITR(IT)=IP
  NCO=NCO+1
  GOTO 210
ELSE IF ((IPA(IP).NE.0).AND.(ITR(IT).EQ.0)) THEN
  ped IP already correlated...
  WRITE(6,*) 'MCCORR: ### DOUBLE CORRELATION'
  WRITE(6,*) IPA(IP),'AND',IT,'HITS SAME XTAL.'
  WRITE(6,*) 'CORRELATION WITH PED NO.:',IP
  ITR(IT)=IP
  NCO=NCO+1
END IF
END IF
LMAX = LQ(LMAX)
GOTO 200
END IF
210 CONTINUE

```

*** Correlation, if max xtal particle +- 1 = max xtal PED

```

* loop over all particles
DO 300 IT = 1,IQ(LMBEN+1)
IF (ITR(IT).EQ.0) THEN
* particle IT not yet correlated ...
** loop over all PEDs
LMAX=LTBTK
IF (LMAX.NE.0) LMAX=LQ(LMAX-1)
310 IF (LMAX.NE.0) THEN
  IF ((IPHP(IT).GE.IQ(LMAX+1)-1).AND.
  & (IPHP(IT).LE.IQ(LMAX+1)+1).AND.
  & (ITHP(IT).GE.IQ(LMAX+2)-1).AND.
  & (ITHP(IT).LE.IQ(LMAX+2)+1)) THEN
* PED#
  IP = IQ(LMAX-5)
  IF (IPA(IP).EQ.0) THEN
* ped IP not yet correlated ...
  IPA(IP)=IT
  ITR(IT)=IP
  NCO=NCO+1
  GOTO 300
  ELSE IF (IPA(IP).NE.0) THEN
  ped IP already correlated ...
  WRITE(6,*) 'MCCORR: ### DOUBLE CORRELATION'
  WRITE(6,*) IPA(IP),'AND',IT,'HITS SAME XTAL.'
  WRITE(6,*) 'CORRELATION WITH PED NO.:',IP
  ITR(IT)=IP
  NCO=NCO+1
  END IF
  END IF
  LMAX = LQ(LMAX)
  GOTO 310
  END IF
  END IF
300 CONTINUE
RETURN
END

```

Appendix II:

List of the SMART cuts as shown in fig. 2 and fig. 3 and used in this analysis:

R_{mass} means the invariant showermass in MeV/c^2 .
 E_{Cluster} is the energy of the whole cluster in MeV.

1. Real clusters:

2 PEDs:

upper cut:

$$R_{\text{mass}} = \frac{7}{80} \cdot E_{\text{Cluster}} + 10$$

lower cut:

$$R_{\text{mass}} = \frac{5}{80} \cdot E_{\text{Cluster}}$$

3 PEDs:

upper cut:

$$R_{\text{mass}} = \frac{14}{50} \cdot E_{\text{Cluster}}, \text{ for } E_{\text{Cluster}} < 500 \text{ MeV}$$

$$R_{\text{mass}} = \frac{6}{70} \cdot E_{\text{Cluster}} + \frac{670}{7}, \text{ for } E_{\text{Cluster}} > 500 \text{ MeV}$$

lower cut:

$$R_{\text{mass}} = \frac{17}{80} \cdot E_{\text{Cluster}}, \text{ for } E_{\text{Cluster}} < 500 \text{ MeV}$$

$$R_{\text{mass}} = \frac{9}{80} \cdot E_{\text{Cluster}} + 80, \text{ for } E_{\text{Cluster}} > 500 \text{ MeV}$$

4 PEDs:

upper cut:

$$R_{\text{mass}} = \frac{28}{100} \cdot E_{\text{Cluster}} + 20$$

lower cut:

$$R_{\text{mass}} = \frac{20}{100} \cdot E_{\text{Cluster}}$$

2. Pseudo clusters:

2 PEDs:

upper cut:

$$R_{\text{mass}} = \frac{7}{80} \cdot E_{\text{Cluster}} + 15$$

lower cut:

$$R_{\text{mass}} = \frac{6}{80} \cdot E_{\text{Cluster}}$$

3 PEDs:

upper cut:

$$R_{\text{mass}} = \frac{19}{80} \cdot E_{\text{Cluster}} , \text{ for } E_{\text{Cluster}} < 560 \text{ MeV}$$

$$R_{\text{mass}} = \frac{9}{80} \cdot E_{\text{Cluster}} + 70 , \text{ for } E_{\text{Cluster}} > 560 \text{ MeV}$$

lower cut:

$$R_{\text{mass}} = \frac{46}{250} \cdot E_{\text{Cluster}} , \text{ for } E_{\text{Cluster}} < 700 \text{ MeV}$$

$$R_{\text{mass}} = \frac{9}{80} \cdot E_{\text{Cluster}} + 50 , \text{ for } E_{\text{Cluster}} > 700 \text{ MeV}$$

4 PEDs:

upper cut:

$$R_{\text{mass}} = \frac{28}{100} \cdot E_{\text{Cluster}} + 20$$

lower cut:

$$R_{\text{mass}} = \frac{20}{100} \cdot E_{\text{Cluster}}$$

These cuts are fixed merely by a careful inspection of the scatterplots shown in fig.2 and fig.3. A fit procedure would certainly yield an improvement on the results in table 3.

